

925

Forecast impact assessment of a potential ATMS instrument in the early-morning orbit using the EDA method

Zaizhong Ma^{1,2}, Niels Bormann², Katie Lean², David
Duncan², Ernesto Hugo Berbery¹ and Satya Kalluri³

¹Cooperative Institute for Satellite Earth System Studies (CISESS) /Earth System Science
Interdisciplinary Center (ESSIC), University of Maryland

²European Centre for Medium-Range Weather Forecasts, Reading, United Kingdom

³NOAA/NESDIS, College Park, USA

December 2024

Series: ECMWF Technical Memoranda

A full list of ECMWF Publications can be found on our web site under:

<http://www.ecmwf.int/publications/>

Contact: library@ecmwf.int

© Copyright 2024

European Centre for Medium Range Weather Forecasts
Shinfield Park, Reading, Berkshire RG2 9AX, England

Literary and scientific copyrights belong to ECMWF and are reserved in all countries. The content of this document is available for use under a Creative Commons Attribution 4.0 International Public License. See the terms at <https://creativecommons.org/licenses/by/4.0/>.

The information within this publication is given in good faith and considered to be true, but ECMWF accepts no liability for error, omission and for loss or damage arising from its use.

Abstract

This study evaluates the impact of a hypothetical future microwave (MW) sounding instrument in a 17:30 Local Time of Ascending Node (LTAN) orbit, in order to provide input to the design of NOAA's future MW sounding missions. As an international collaborative effort between the University of Maryland Cooperative Institute for Satellite Earth System Studies (UMD/CISESS) and the European Centre for Medium-Range Weather Forecasts (ECMWF), the potential Numerical Weather Prediction (NWP) benefits of these future MW sounders are being evaluated using an Ensemble of Data Assimilations (EDA) approach. The EDA method for assessing new observations provides a theoretical estimate of the expected reduction in analysis and short-range forecast uncertainty, as a result of assimilating the new data. A reduction of the spread resulting from additional observations used is hence an indication of beneficial impact from these observations. This study focuses on assessing the impact of an Advanced Technology Microwave Sounder (ATMS)-like instrument in a 17:30 LTAN orbit (referred to as 1730_LTAN), comparing its performance to existing sounders on the Polar Operational Environmental Satellites (POES) and ATMS instruments in the 13:30 LTAN orbit. For the new 1730_LTAN instrument, we assume a performance similar to that of ATMS on Suomi National Polar-orbiting Partnership (S-NPP).

The EDA analysis shows that 1730_LTAN significantly impacts a range of atmospheric variables, when added on top of an observing system that uses MW-sounders from Meteorological Operational satellite (Metop) and Joint Polar Satellite System (JPSS) satellites only, but otherwise includes all other operationally used observations. The impact of a MW sounder in 1730_LTAN orbit is similar to or slightly larger than the benefit currently achieved with real data from the remaining MW-sounding instruments on the POES satellites (NOAA-15, 18, and 19), and the largest impact is achieved when 1730_LTAN and POES satellites are used together. When added to NOAA's contribution from the JPSS system — including the Cross-track Infrared Sounder (CrIS), the Visible Infrared Imaging Radiometer Suite (VIIRS), and ATMS from S-NPP and NOAA-20 — the 1730_LTAN MW sounder provides an additional increase the overall short-range forecast impact.

Sensitivity experiments that assume a degraded noise performance for the temperature-sounding channels of 1730_LTAN show that the benefit is significantly reduced compared to assuming S-NPP like noise levels, though some benefits from adding these observations are still observed. These findings emphasize the importance of instrument noise characteristics for the effectiveness of microwave temperature sounding observations in NWP systems.

In addition, the consistency of the impact in the EDA between real and simulated microwave radiance observations is also evaluated. An additional experiment was conducted to compare the impact of simulated ATMS data with that of real ATMS observations from S-NPP and NOAA-20 satellites. The results show that the simulated and real ATMS data have a similar impact on EDA spread, suggesting that the simulations provide realistic predictions of actually achieved impact in the EDA.

Plain Language Summary

In this study we investigate the benefit for weather forecasting from adding a hypothetical new satellite instrument to the global observing system (referred to as 1730_LTAN). The additional satellite flies in a sun-synchronous polar orbit, observing the globe in the late afternoon/early morning. The instrument

is a microwave (MW) sounder, that is, it provides measurements of the Earth's radiation in the MW spectrum, aimed at obtaining information on temperature and humidity profiles. It is assumed to have the characteristics similar to the ATMS sensor on the Suomi-NPP satellite. The new data is first simulated from high-resolution ECMWF analyses. Monte-Carlo methods are then used to estimate the change in the uncertainty in short-range (12h) global weather forecast arising from adding the new data to a set of existing observations, employing a system known as Ensemble of Data Assimilations (EDA).

The results show that significant benefit would be expected for short-range forecasts from adding 1730_LTAN to an observing system that features MW sounding from satellites in the morning (Metop) and afternoon (JPSS) orbits only, but otherwise includes all other operationally used observations. The impact is comparable to that of current POES satellites, with the greatest improvements observed when data from 1730_LTAN and the POES satellites are combined. Additional experimentation shows that the accuracy of the data from the 1730_LTAN instrument is important, and the beneficial impact is significantly reduced if the instrument noise is larger, i.e. the measurements are less accurate.

By comparing the impact seen from simulated ATMS data from the S-NPP and NOAA-20 with that of real data, we highlight that the estimated impacts are similar, suggesting that the simulations provide realistic predictions of actually achieved impact in the EDA.

1. Introduction

Satellite observations from microwave-sounding instruments significantly impact global Numerical Weather Prediction (NWP) and are essential elements of the global observing system (Bormann et al., 2019). These instruments provide all-weather sounding capabilities for temperature and humidity and offer indirect information on wind, which can be leveraged in modern data assimilation systems. Over the years, the European Centre for Medium-Range Weather Forecasts (ECMWF) has developed advanced applications of microwave sounding observations for NWP, particularly regarding the all-sky usage of these observations (Geer et al., 2017) and the variety of instruments employed (Bormann et al., 2013; Lawrence et al., 2018).

The benefits of having high-quality observations from multiple orbits have been well established, including the ongoing contributions of the heritage Polar Operational Environmental Satellites (POES) series (Duncan et al., 2021). The complementarity of the equator-crossing times plays a particular role to optimise this impact. Using data from the Fengyun-3 (FY-3) series or POES satellites, Steele et al (2023) and di Tomaso and Bormann (2011) showed that instruments added in an orbit not previously covered tend to have a larger impact than instruments added in an orbit that is already covered by other similar instruments. This experience is also highlighted in the significant positive impact obtained from the recent introduction of the FY-3E satellite in the early-morning orbit, an orbit that was previously not well covered (e.g., Steele et al 2023, Xiao et al 2023). In alignment with these experiences, the World Meteorological Organization (WMO) Vision for the Global Observing System envisions microwave sounding capabilities from three complementary backbone polar orbits, augmented by additional orbits to enhance temporal sampling. Given the critical role of microwave sounding in NWP, ensuring that future capabilities of the backbone three-orbit constellation meet stringent requirements is of utmost importance for advancing forecast performance.

National Oceanic and Atmospheric Administration (NOAA) has a long history of successfully operating environmental satellites in low-Earth orbit (LEO) for over 50 years. Figure 1 illustrates the progression of NOAA's LEO weather satellites. The Office of LEO Observations at NOAA encompasses two programs: the Joint Polar Satellite System (JPSS) and the Near Earth Orbit Network (NEON). The JPSS satellites orbit Earth from pole to pole, crossing the equator 14 times daily in the afternoon orbit, providing full global coverage twice a day and supporting operational forecasting. The NEON program sets the stage for NOAA to manage future LEO environmental satellites, which will supplement and eventually replace JPSS.

The first project in the NEON Program series is QuickSounder, expected to launch in 2026. This pathfinder mission aims to demonstrate NOAA's ability to launch a small satellite within three years. QuickSounder will carry a refurbished Advanced Technology Microwave Sounder (ATMS) instrument, similar to those on the Suomi National Polar-orbiting Partnership (S-NPP) satellite, NOAA-20 (formerly JPSS-1), NOAA-21 (formerly JPSS-2), and further JPSS satellite missions. Notably, QuickSounder will be launched into an early-morning orbit, a capability currently lacking in the US/Europe Joint Polar System.

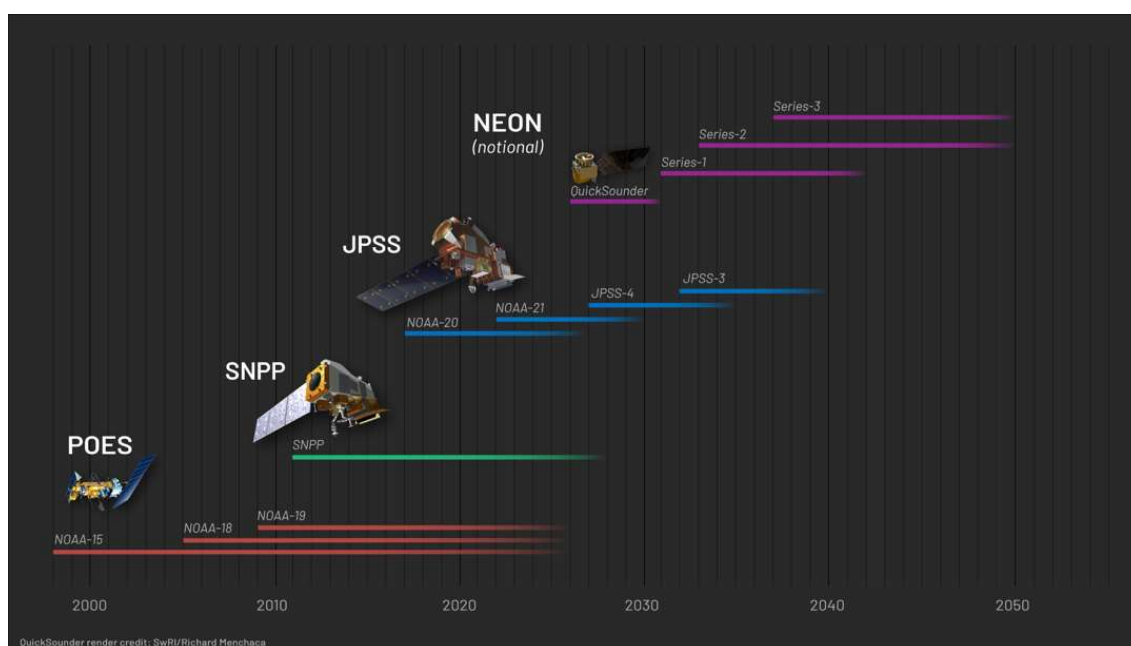


Figure 1: Chart showing the progression of NOAA's low earth orbit weather satellites, with the NEON Program conceptualized. More details please find from the website: <https://www.nesdis.noaa.gov/our-satellites/future-programs/near-earth-orbit-network-neon>.

Research is required to assess how advances in satellite systems translate to improved weather forecasts, to guide design choices and lead to cost-effective systems. To evaluate the expected impact of future satellite missions, ECMWF has developed the Ensemble of Data Assimilations (EDA) approach (Tan et al., 2007; Isaksen et al., 2010). The EDA estimates random uncertainty by representing errors in observations, models, and input fields such as sea surface temperatures through appropriate perturbations using a Monte-Carlo approach. Provided that the perturbations adequately represent actual statistical errors, the ensemble spread reflects the random statistical uncertainty in analyses and forecasts. A reduction in ensemble spread resulting from additional observations indicates a beneficial

impact from these observations. To conduct EDA experiments, new observations and their expected error characteristics are simulated and used alongside the existing observing system. This method serves as an alternative to Observing System Simulation Experiments (OSSEs), where all assimilated observations and their error characteristics must be simulated. The requirement to simulate only new observations is a significant advantage. The EDA method has previously been employed to estimate the expected impact of the Doppler Wind Lidar Aeolus (Tan et al., 2007; Healy et al., 2023) and to evaluate increases in the number of provided radio occultation data (Harnisch et al., 2013). The most recent application of the EDA method assessed the potential impact of future constellations of small satellites carrying microwave sounding instruments, in collaboration with the European Space Agency (ESA) and the European Organisation for the Exploitation of Meteorological Satellites (EUMETSAT) (Lean et al., 2022, 2023). This application demonstrated that the positive impact of adding more microwave sounding observations continued to increase, although for large constellations (20 small satellites), the gain in benefit began to level off (Lean et al., 2022).

In this study, we evaluate the NWP impact of an ATMS instrument in a sun-synchronous orbit with a 17:30 Local Time of Ascending Node (LTAN) using the EDA approach. The instrument is assumed to have a similar performance as the ATMS on S-NPP, and we will refer to this instrument as “1730_LTAN” throughout the study. Following previous work by Lean et al. (2022, 2023), a framework has been adopted to simulate and assimilate microwave sounding data from 1730_LTAN. A series of scenarios for the 1730_LTAN EDA impact studies are performed over the period from 1 to 30 June 2021, consisting of three addition experiments and two denial experiments relative to a reference baseline. The baseline observing system serves as a proxy for future NOAA microwave sounding measurements and includes all non-microwave observations utilized by ECMWF in 2021, excluding passive microwave data from Micro-Wave Humidity Sounder-2 (MWHS-2) and Special Sensor Microwave - Imager/Sounder (SSMIS). The study is a collaborative effort between the University of Maryland Cooperative Institute for Satellite Earth System Studies (UMD/CISESS) and ECMWF.

The efficacy of MW sounders depends upon their noise levels, both those of individual channels (given by noise-equivalent differential temperature or NEDT) and correlated noise between channels (Qin et al., 2013; Biswas et al., 2024). A poorer noise performance will lead to a reduced impact, particularly for temperature-sounding channels. In this study, we investigate the sensitivity of the NWP impact to the noise performance of the 1730_LTAN instrument. Building on prior work (Lean et al., 2023), we conduct an experiment where the NEDT values are increased by 100% for channels 1-10 and by 50% for channels 11-15. Corresponding adjustments are made to the observation error values to simulate a scenario with degraded noise performance. This additional experiment provides valuable insights into how poorer instrument noise might affect the assimilation of microwave observations and the overall impact on NWP performance.

In addition to assessing the impact of 1730_LTAN on NWP, an additional experiment is conducted to evaluate the similarity between simulated and real ATMS data in the EDA framework. This experiment aimed to assess the consistency of real and simulated microwave radiance observations in the EDA system. To achieve this, ATMS measurements from S-NPP and NOAA-20 are simulated at the respective observation times and locations, utilizing ECMWF operational analysis, ATMS simulation code, and observational uncertainty models.

This report is structured as follows: Section 2 provides an overview of the key aspects of the EDA approach and previous EDA studies used to evaluate new observing systems at ECMWF. Section 3 discusses the observational properties of a ATMS in a 1730_LTAN, reviewing the framework developed by Lean et al. (2022, 2023) and any modifications enabling flexible simulation and assimilation of 1730_LTAN microwave data. The experiment setup is shown in Section 4, and then section 5 presents the results of the EDA experiments, including an additional experiment to estimate the similarity between simulated and real ATMS data in the EDA system. In addition, Section 5 includes results from another experiment designed to evaluate the sensitivity of NWP performance to instrument noise. Finally, Section 6 discusses the conclusions of the first part of this study and outlines plans for Sounder for Microwave-Based Applications (SMBA) EDA experiments.

2. Ensemble of Data Assimilation method

The Ensemble of Data Assimilations (EDA) method has been a vital component of the ECMWF IFS system since 2010, assisting in determining initial conditions for ensemble forecasts (ENS) and higher-resolution deterministic forecasts (HRES) (Isaksen et al., 2010; Bonavita et al., 2016; Lang et al., 2019). Employing a Monte-Carlo approach, EDA estimates the statistical characteristics of errors in analyses and short-range forecasts by addressing uncertainties in input parameters and the forecast model. Its primary role within the IFS is to contribute to the representation of initial condition uncertainties in the ENS system while providing flow-dependent uncertainty information in the HRES system.

The EDA method offers an accessible and manageable framework for assessing the impact of future observing systems (Bormann et al., 2023; Healy et al., 2024). By evaluating changes in EDA spread, this method provides estimates on how potential future observations may affect analysis and short-range forecast error statistics. A reduction in EDA spread, which indicated by the ensemble's standard deviation around the mean, shows a positive impact, reflecting improved forecast accuracy. This ability to quantify how new or proposed observations affect forecast uncertainty makes EDA a valuable tool for optimizing observing systems and evaluating the potential benefits of future satellite missions or instrumentation upgrades. Note that the ensemble spread is a crucial measure of the EDA, i.e. the standard deviation of the ensemble members around the ensemble mean as given in the following equation:

$$s = \sqrt{\frac{1}{D} \sum_{d=1}^D \left[\frac{1}{N-1} \sum_{n=1}^N (x_n - \bar{x})^2 \right]_d} \quad (1)$$

Where s is the spread, D is the required time period e.g. the number of model cycles, N is the size of the ensemble (10 members for this study), x_n is the model state from a single ensemble member and \bar{x} is the ensemble mean.

The EDA method has been applied to various mission types prior to launch at ECMWF over the years. Tan et al. (2007) first utilized the method to assess the expected impact of wind profile observations from Aeolus, demonstrating that the assimilation of simulated Aeolus measurements reduced ensemble spread, thereby estimating the impact of the measurements. Harnisch et al. (2013) subsequently employed EDA to evaluate how the impact of Global Navigation Satellite System (GNSS) Radio

Occultation (RO) observations scales with the number of observations. More recently, Lean et al. (2022, 2023) applied EDA to investigate a potential constellation of small satellites equipped with microwave (MW) instruments. In the present study, this well-established EDA framework at ECMWF will be utilized to evaluate the benefits of the proposed 1730_LTAN MW sounder, an ATMS-like mission in the 17:30 LTAN orbit.

While EDA and traditional Observing System Simulation Experiments (OSSEs) share the goal of measuring the expected impacts of future observing systems, they differ conceptually. OSSEs involve extensive computational requirements, including high-resolution “nature runs” (NR) to represent the true atmospheric state and the simulation of all existing observing systems (Atlas et al., 2015; Ma et al., 2015; Errico and Privé, 2018). In contrast, EDA offers a cost-effective alternative, as it can utilize both real and simulated observations. Moreover, EDA directly benefits from refinements made in background-error modeling within operational numerical weather prediction (NWP) systems. The main differences of side-by-side comparisons between OSSEs and EDA are shown in Table 1.

Table 1: Complementary approaches for future mission impact study: Observing System Simulation Experiments (OSSEs) and Ensemble of Data Assimilations (EDA) techniques.

Methods	OSSEs	EDA
Observations	Simulate all observations from known truth – “nature run”	Simulate new observations only and add to existing baseline
Systems	Assimilate in NWP system and compare to known nature run	Assimilate in EDA system and compute spread across EDA members
Evaluations	Compute statistics of analysis/forecast errors, including for medium-range forecasts	Estimates analysis/short-range forecast error covariance matrices i.e. PDF of errors, not actual forecast errors

3. 1730_LTAN and its Observation Simulation and Assimilation

3.1. Instrument characteristics

This study conducts a series of EDA experiments for 1730_LTAN, an ATMS instrument with a performance similar to the one on S-NPP, but with a 17:30 LTAN. Like other ATMS instruments, 1730_LTAN will measure microwave radiances across 22 channels (ranging from 23.8 GHz to 183.3 GHz), enabling temperature soundings from the surface to the upper stratosphere (up to about 1 hPa, approximately 45 km altitude) and humidity soundings from the surface to the upper troposphere (up to about 200 hPa, roughly 15 km altitude). 1730_LTAN will employ a cross-track scanning mechanism, featuring two receiving apertures: one for 15 channels below 60 GHz with a beam width of 2.2°, and another for seven channels above 60 GHz with a beam width of 1.1° (excluding the lowest channel frequency). Table 2 summarizes the 1730_LTAN performance specifications of all 22 channels, including radiometric sensitivity, which is usually called NEDT.

Table 2: 1730_LTAN spectrometric and radiometric characteristics. The values for the NEDT are based on typical in-flight values for S-NPP, adopted for 1730_LTAN in this study.

Channel Number	Passband Center Frequency (GHz)	Polarization near nadir	Number of Passbands	NEDT (K)	Primary Function
1	23.8	vertical	1	0.24	Water Vapor Burden
2	31.4	vertical	1	0.32	Water Vapor Burden
3	50.3	horizontal	1	0.36	Surface Emissivity, Precipitation
4	51.76	horizontal	1	0.28	Tropospheric Temperature
5	52.8	horizontal	1	0.25	Tropospheric Temperature
6	53.596 ± 0.115	horizontal	2	0.28	Tropospheric Temperature
7	54.4	horizontal	1	0.25	Tropospheric Temperature
8	54.94	horizontal	1	0.25	Temperature Near Tropopause
9	55.5	horizontal	1	0.28	Temperature Near Tropopause
10	57.290344	horizontal	1	0.40	Stratospheric Temperature
11	57.290344 ± 0.217	horizontal	2	0.54	Stratospheric Temperature
12	57.290344 ± 0.3222 ± 0.048	horizontal	4	0.56	Stratospheric Temperature
13	57.290344 ± 0.3222 ± 0.022	horizontal	4	0.84	Stratospheric Temperature
14	57.290344 ± 0.3222 ± 0.010	horizontal	4	1.15	Stratospheric Temperature

15	$57.290344 \pm 0.3222 \pm 0.0045$	horizontal	4	1.84	Stratospheric Temperature
16	88.2	vertical	1	0.25	Clouds/Snow
17	165.5	horizontal	1	0.40	Water Vapor
18	183.31 ± 7.0	horizontal	2	0.36	Water Vapor
19	183.31 ± 4.5	horizontal	2	0.45	Water Vapor
20	183.31 ± 3.0	horizontal	2	0.50	Water Vapor
21	183.31 ± 1.8	horizontal	2	0.56	Water Vapor
22	183.31 ± 1.0	horizontal	2	0.69	Water Vapor

3.2. Observation Simulation and Assimilation

In this section, we first introduce the all-sky assimilation of ATMS for both simulation and assimilation within the ECMWF system (Cycle 48r1). We then briefly outline the key steps of the simulation framework for future NOAA MW missions, based primarily on ESA and EUMETSAT contract reports (Lean et al., 2022, 2023) for detailed information.

3.2.1. All-sky assimilation of ATMS

The all-sky assimilation of MW radiances has been developed at ECMWF over several years (e.g., Geer et al., 2017). In this approach, observations are assimilated in clear, cloudy and rainy conditions, and model cloud fields are used in the observation operator. This has been shown to provide a larger impact than the previous approach of assimilating observations in clear-sky conditions only, particularly for humidity-sensitive microwave radiances. Any new MW instrument is now assimilated using the all-sky approach from the start, whereas older instruments are gradually moved to this approach. Currently, ATMS is the only remaining sensor that is still used under clear-sky conditions in the operational ECMWF system.

For better consistency across different instruments, the present study adopts an all-sky assimilation approach for all MW instruments, including ATMS, using a prototype system expected to become operational in the future. This brings the use of ATMS in line with that of other MW sounding instruments. Aside from using data in clear, cloudy and rainy conditions and an all-sky observation operator, the key differences compared to the clear-sky approach are: 1) A different approach is used for spatial thinning, favoring regular spatial sampling according to a T_L159 Gaussian grid (~125 km resolution) rather than clear-sky regions; 2) Inter-channel error correlations are not explicitly taken into

account, but instead ad-hoc inflation of assigned observation errors is used, and 3) Lambertian effects over snow and sea ice are not taken into account and instead a specular assumption is used. The all-sky assimilation of ATMS follows the examples of existing instruments sounders used in the all-sky framework. The temperature-sounding channels are thus assimilated following Duncan et al. (2022), with the humidity-sounding channels following Geer et al. (2014). Radiances from both sets of channels are used over most surfaces with specific exceptions outlined by Geer et al. (2022).

3.2.2. *Simulating 1730_LTAN MW brightness temperatures*

The EDA computations rely on a simulated dataset produced by a system depicted in Figure 2. The simulation framework for NOAA's future 1730_LTAN MW missions consists of three essential steps: 1) interpolating high-resolution atmospheric data to observation locations, 2) converting atmospheric data into brightness temperatures (BTs) using a radiative transfer model (RTTOV-SCATT), and 3) adding random noise to mimic realistic instrument performance.

This framework builds on earlier work by Lean et al. (2022) for potential future MW-sounding constellations, and replicates as far as possible the simulation of model-equivalents performed as part of the operational all-sky assimilation of MW radiances. The study uses high-resolution ECMWF analysis trajectories (TCo1279, approximately 9 km, 137 vertical levels) as a proxy for the true atmospheric state. Spatial and temporal sampling for the model fields is based on simulations of ATMS scan-pattern for the 17:30 LTAN orbit, kindly provided by EUMETSAT. RTTOV-SCATT (version 13.2) is employed for radiative transfer modelling, accounting for hydrometeor scattering at MW frequencies, enabling the use of MW data in an all-sky context (Saunders et al., 2020; Geer et al., 2021).

The simulated observations are sub-sampled to simulate the effect of super-obbing and spatial thinning. For the assimilation of real ATMS data, 9 observations from 3 adjacent scan-positions and 3 scan-lines are averaged ("3x3 averaging"), in order to reduce the effective instrument noise, which is particularly crucial for the temperature-sounding channels. The effect is simulated here by selecting only every 3rd scan-position and every 3rd scan-line and taking the noise-reduction effect into account in the uncertainty modelling of the simulated observations (see below). This initial selection is then followed by retaining only the super-obbed observations closest to a T_L159 Gaussian grid (~125 km) within a 30-minute timeslot, as applied in the all-sky assimilation of real ATMS data.

Perturbations are added to the simulated observations to capture real instrument performance, accounting for varying NEDT between temperature and humidity channels. The perturbations sample Gaussian random noise with a mean of zero and a standard deviation that aims to take into account the effect of the 3x3 averaging applied. For white noise, the 3x3 averaging would imply a reduction of the NEDT by a factor of 3. However, ATMS exhibits considerable contributions of 1/f noise (e.g., Kim et al., 2014). This results in a less effective noise-reduction of the 3x3 averaging. To take this effect into account, we instead apply the noise-reduction factors derived empirically by Weston et al (2018) for the S-NPP ATMS. These factors are around 2.4 for the tropospheric temperature-sounding channels and around 2 for the humidity-sounding channels. The effective noise is hence given by the NEDT values shown in Table 2, divided by these factors. Note that no attempt is otherwise made to simulate striping effects that have been observed particularly for the S-NPP ATMS (Bormann et al., 2013). Also not included in the observation simulation are systematic errors, arising, for instance from calibration or radiative transfer errors.

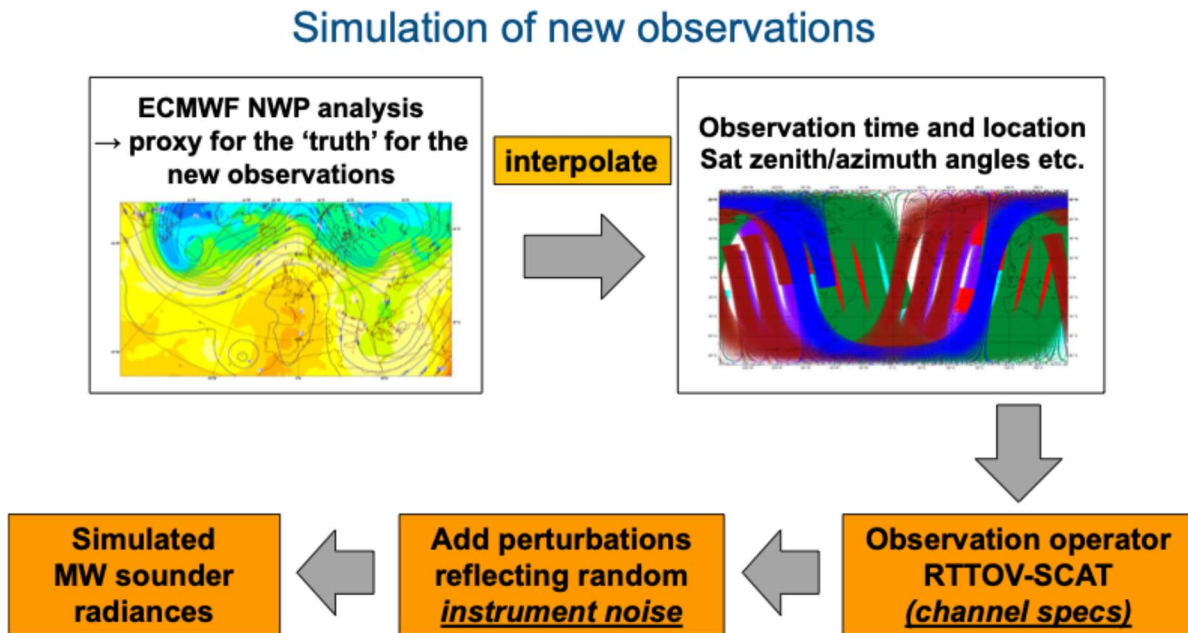


Figure 2: Standard simulation system used to generate observations for EDA computations. It is important to note that errors are introduced both during this simulation step and subsequently in the EDA process. The simulated 1730_LTAN data has been produced using this standard simulation system.

3.2.3. Observation error and data assimilations

The observation error model for 1730_LTAN data during assimilation follows ECMWF’s all-sky approach, where the assigned observation error increases in the presence of cloud signals detected in either the observations or the model (Geer and Bauer 2011). This approach has been used effectively for existing microwave (MW) instruments. In cloudy conditions, errors are dominated by differences between the clouds represented in the observations and the model fields, whereas in clear-sky regions the instrument noise plays a larger role. The observation error model is formulated as a function of a symmetric cloud indicator, using an estimate of the liquid water path based on Grody et al. (2001) for the temperature-sounding channels, and a scatter index based on the 89 and 165 GHz channel for the humidity-sounding channels.

Key parameters of the observation error model are the value assigned to clear-sky regions and the value assigned for cloudy regions for each channel. These values have been set empirically based on standard deviations of departures between real S-NPP ATMS observations and the model background as outlined by Geer et al. (2011). Resulting values for the clear-sky observation error are in-line with values obtained with empirical formulae proposed by Lean et al. (2022) to link the assigned value to the effective NEDT. In addition, an ad-hoc empirical adjustment to the assigned observation error is introduced here to partially compensate for neglecting inter-channel error correlations in the all-sky use of ATMS. As outlined by Bormann et al. (2013) and Weston and Bormann (2018), the ATMS instrument noise is correlated between different channels, and this effect is larger for the S-NPP ATMS. To reduce the effect of neglecting these error correlations in the assimilation, we inflate the assigned clear-sky observation error by the square root of the leading eigen-value of the inter-channel error

correlation matrix. There is no accurate way to determine the appropriate inflation, but the factor is chosen to reduce the over-weighting of the leading eigen-structures that otherwise occurs.

Once the simulated BTs have been processed through thinning and noise perturbations, they are ready for assimilation in EDA experiments. Quality control choices for 1730_LTAN are the same as those applied to real ATMS data, and key settings are provided in Table 3. Bias correction is handled through the variational bias correction (VarBC) scheme, ensuring the 1730_LTAN does not act as anchor observations. Each channel on the 1730_LTAN instrument receives separate bias corrections, consistent with real MW data treatments.

Table 3: Summary of key quality control and processing choices made in the assimilation of MW radiances on the existing MW sounders. (Adapted from Lean et. al., 2023)

Assimilation choice	Application to all-sky MW
Radiative transfer model	RTTOV-SCATT v13 (Saunders et al., 2020; Geer, 2021)
Ocean emissivity	FASTEM-6 (Kazumori and English, 2015)
Land/sea ice emissivity	Dynamic retrieval using 50.3GHz for temperature sounding, 165.5GHz for humidity sounding (Karbou et al., 2006; Baordo and Geer, 2016)
Tropics (<30° N/S) orography rejection	53.246 and 53.596 GHz height < 1000m, 54.4GHz height < 2000m
Extratropics orogra- phy rejection	53.246 and 53.596 GHz height < 500m, 54.4GHz height < 1500m
Polar regions (>60° N/S)	53.246, 183±7 and 183±4.5 GHz rejected over all surfaces, 53.596 GHz rejected over land/sea ice in Antarctic region only
Coast	53.246, 53.596, 54.4, 183±7 and 183±4.5 GHz rejected
Snow/sea-ice	53.246, 183±7 and 183±4.5 GHz rejected
Surface sensitive channel rejection	23.8, 31.4, 50.3, 52.8, 89 and 165.5 GHz not directly assimilated (but used e.g. in emissivity and observation error calculation)

4. EDA Experiments setup

The EDA experiments in this study follow a standard configuration used at ECMWF for operational development testing and future observing systems assessments. The setup includes one control member

and 10 perturbed members, running on a TCo399 (25 km) resolution grid with 137 vertical levels and three inner loops at resolutions of TL95/TL159/TL255 (210/125/80 km). These experiments span the period from 1 to 30 June 2021, a time when key MW instruments and other observing system components were stable and performing well. After discarding the first week’s data, in order for the EDA spread to where the EDA develops representative levels of spread during this spin-up time, the remaining three weeks are sufficient to provide robust estimates of EDA spread changes (Lean et al., 2021a,b). The spread changes are calculated at TL255 resolution and T+12 hours, as shorter lead times provide clearer signals (Lean et al., 2021a,b). This setup enables the assessment of spread reductions due to the addition of 1730_LTAN satellite data, evaluating impacts under various scenarios.

The Baseline observing system used in this study employs the full global observing system used operationally at ECMWF in June 2021, but with MW-sounding from two backbone polar orbits only, that is, the early morning covered by Meteorological Operational satellite (Metop) satellites and the afternoon orbit covered by S-NPP and NOAA-20 (Table 4). The passive MW data from China’s FY-3C and D satellites (MWHS-2) and sounding channels from two SSMIS instruments are excluded. The motivations for these exclusions are two-fold: 1) they reflect expected limitations in future satellite programs (e.g., sounding capabilities on SSMIS-successors are not maintained, POES satellites are not maintained), 2) some US NWP centres are not allowed to use certain observations due to their own data policy issues.

Table 4: Baseline Observing System

Included in Baseline Observing System	All non-MW observations used operationally at ECMWF at the time	In-situ/surface-based observations from sondes, profilers, synops, aircraft, etc
		Hyperspectral IR from AIRS, 2 IASI, 2 CrIS
		GPSRO from COSMIC-2, 2 GRASS, SPIRE, GRACE-C, KOMPSAT-5, TANDEM-X, TERRASAR-X, Sentinel-6a
		Geo-radiances from GOES-16, -17, Meteosat-9, -11, Himawari-8
		Doppler Wind Lidar data from Aeolus
	Atmospheric Motion Vectors (AMVs) from geostationary and polar satellites	
	A set of MW instruments	MW sounders from 2 Metop satellites – i.e. only one orbit with cross-track MW sounders
		JPSS ATMS from S-NPP and NOAA-20
		AMS2, GMI, SSMIS (window channels only)

Excluded observations	Passive MW data from MWHS-2 on FY-3C and D.
	Sounding channels from two SSMIS instruments – not maintained in future DoD program

Table 5: A detailed list of proposed scenarios in 1730_LTAN EDA impact studies.

Scenario Name	Observing system other than MW sounding	MW sounding in 9:30 orbit	MW sounding in 13:30 orbit	MW sounding in 17:30 orbit	Further MW sounding
No JPSS	CrIS & AMVs from S-NPP & NOAA-20 denied, otherwise full	Two Metop	-	-	-
No ATMS*	Full	Two Metop	-	-	-
Baseline	Full	Two Metop	Two ATMS (S-NPP, NOAA-20)	-	-
Baseline+POES**	Full	Two Metop	Two ATMS (S-NPP, NOAA-20)	-	AMSU-A: NOAA-15, -18, -19 MHS: NOAA-19
Baseline+1730_LTAN	Full	Two Metop	Two ATMS (S-NPP, NOAA-20)	1730_LTA N	-
Baseline+POES+1730_LTAN	Full	Two Metop	Two ATMS	1730_LTA N	AMSU-A: NOAA-15, -18, -19

			(S-NPP, NOAA-20)		MHS: NOAA-19
--	--	--	---------------------	--	--------------

*No ATMS on JPSS series used in the assimilation experiment, but CrIS and VIIRS AMVs are used.

** In mid-2021, the LTANs for the POES satellites were approximately as follows: NOAA-18 had an LTAN of 22:00, similar to that of the Metop satellites, while NOAA-15 and NOAA-19 had LTANs around 19:30.

This study involves denial experiments to assess the impact of removing components from the baseline observing system and addition experiments to evaluate the effect of adding new components. Two denial and three addition scenarios are detailed in Table 5. Aside from the addition of simulated 1730_LTAN data, the experiments also include the addition or denial of real observations (e.g., POES data), to provide further context. One EDA experiment is run for each of the scenarios listed in Table 5.

5. Validation of methods

In this section, we first compare simulated 1730_LTAN data with real ATMS observations, to evaluate the realism of the simulations. Subsequently, we present an additional experiment assessing the similarity between real and simulated ATMS data in the EDA, which provides insights into the reliability of the simulation and its implications for operational forecasting.

5.1. Cross-check in DA

To ensure the accuracy of the simulated 1730_LTAN data, we compared observations and departure statistics for simulated 1730_LTAN BTs with those from the S-NPP ATMS instrument, using a 4D-Var experiment in which the simulated 1730_LTAN data were added. Figure 3 present the spatial distribution maps of BTs (left panels) and background departures (right panels) for temperature channel 6 on S-NPP ATMS and 1730_LTAN separately. The maps show the sample of used data, that is, after thinning and geographical quality control has been applied.

The results show that the BT distributions and departures are highly similar, confirming that the 1730_LTAN simulations indeed show a high degree of realism. This is consistent with previous findings of Lean et al (2022) who also showed that departure statistics for simulated and real data exhibit a good consistency. For some regions, data are excluded due to quality control for poorly modelled surface contributions for this surface-sensitive channel, such as sea-ice regions or areas with high-orography, and there is good consistency of these. Note that the geographical locations sampled by the two instruments differ as expected, a result of the different over-pass times (17:30 for 1730_LTAN and 13:30 for S-NPP).

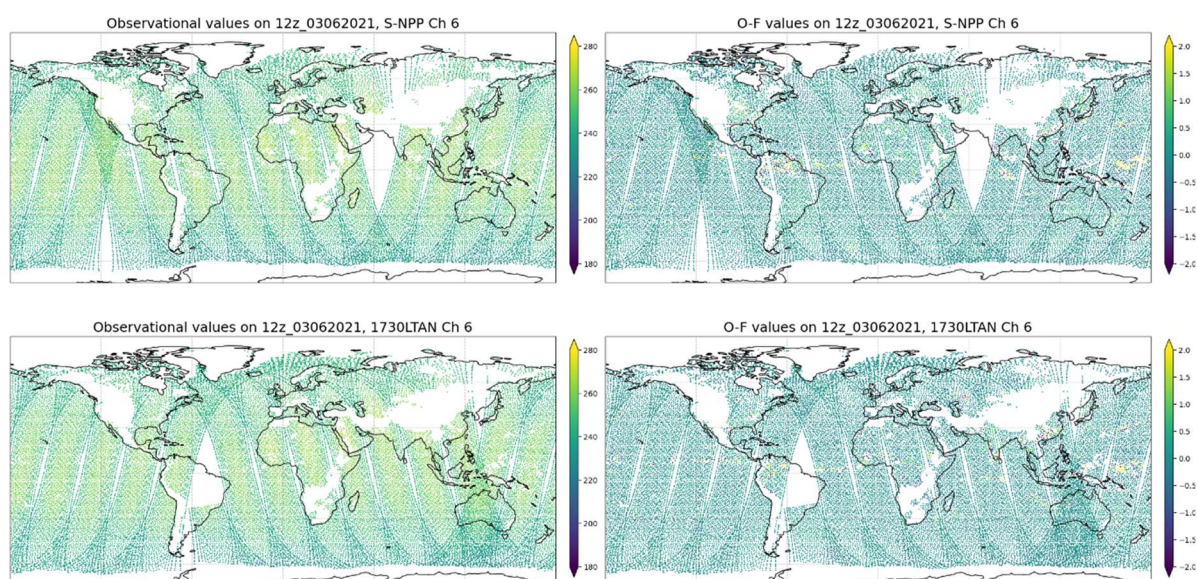


Figure 3: Cross-check of Brightness Temperatures within the IFS data assimilation system. The assimilation cycle picked up here is from 12z, 03 June 2021. The left panels show observational or simulated BTs, while the right panels present the incremental values (O-F), representing the difference between observations and the first guess. The top two panels display results from the S-NPP ATMS instrument, and the bottom two panels correspond to 1730_LTAN's simulated data for Temperature Channel 6. Despite differences in orbital configurations (afternoon orbit for S-NPP and early morning orbit for 1730_LTAN), the BT distributions exhibit high similarity.

This cross-check serves as a critical validation step, confirming the accuracy of the 1730_LTAN data simulation system. With this assurance, we proceeded with greater confidence to conduct the EDA experiments using the simulated 1730_LTAN data, knowing that any observed impacts in the forecast system would be attributable to the inherent characteristics of the instrument, rather than potential issues in the simulation process.

5.2. Similarity of real and simulated ATMS in the EDA

To further evaluate the approach adopted here to simulate the expected impact of 1730_LTAN ATMS data, we have also compared the effects of real and simulated ATMS measurements within the EDA system. To do so, simulated data was generated for the ATMS on the S-NPP and NOAA-20 satellites, with both datasets processed using orbital parameters corresponding to the actual ATMS data collected during 2021. An additional EDA experiment was conducted using this simulated S-NPP and NOAA-20 ATMS data, referred to as SIMU_ATMS, which is detailed in Table 6. By comparing the spread reductions from both the REAL_ATMS (which is same as the Baseline in Table 5) and SIMU_ATMS experiments against the No ATMS scenario (also same as that in Table 5), we can assess how effectively the simulated data replicates the spread reduction achieved with real data.

Table 6: A detailed list of scenarios for ATMS similarity EDA impact studies.

Scenario Name	Observing system other than MW sounding	MW sounding in 9:30 orbit	MW sounding in 13:30 orbit	MW sounding in 17:30 orbit	Further MW sounding
No ATMS (Same as that in Table 5)	Full	Two Metop	-	-	-
REAL_ATMS (Same as Baseline in Table 5)	Full	Two Metop	Two Real ATMS (S-NPP, NOAA-20)	-	-
SIMU_ATMS	Full	Two Metop	Two Simulated ATMS (S-NPP, NOAA-20)	-	-

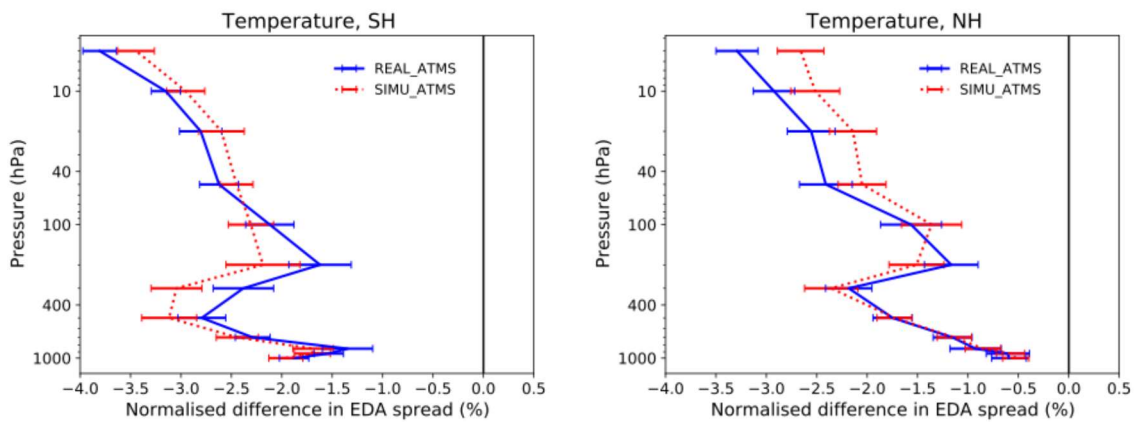


Figure 4: Vertical profiles of EDA spread reduction for temperature in the southern and northern hemisphere from the real and simulated ATMS scenarios.

Figure 4 presents the vertical profiles of the 12-hour forecast temperature spread reductions derived from both real and simulated ATMS data. The comparison demonstrates a strong agreement between the spread reductions obtained with the two datasets. Some small differences are notable, such as a larger spread-reduction in the troposphere for the simulated data over the Southern Hemisphere and a larger spread reduction for the real data in the stratosphere over the Northern Hemisphere. However, overall, the results are in remarkable agreement. In addition to temperature, we observe similar consistency in the results for geopotential, wind, and relative humidity (not shown). These outcomes suggest that the simplifications and approximations applied during the ATMS simulation process

(described in Section 3.2.2) have a relatively small influence on the EDA spread estimates. As such, we can reasonably predict the performance of real ATMS data based on the simulated versions.

The results are also in agreement with findings from Healy et al. (2023), which compared real and simulated Aeolus Doppler Wind Lidar data in the EDA. Their study reported similarly alignment between the two datasets, further supporting the validity of simulation-based evaluations. The consistency observed in both studies demonstrates the robustness of these methodologies for simulating satellite data and assessing their impact on NWP.

6. Results

This section examines the EDA performance of 1730_LTAN by comparing results from denial and addition experiments, shedding light on the incremental benefits of incorporating 1730_LTAN observations into the assimilation system. Additionally, a separate experiment is designed to evaluate the sensitivity of NWP performance to instrument noise. By modifying the NEDT values for the temperature-sounding channels of the 1730_LTAN instrument, this experiment simulates a scenario with degraded noise performance, helping to determine how changes in noise levels may impact the assimilation of microwave observations in NWP.

6.1. EDA results

In this sub-section, we present the results of the EDA experiments conducted to evaluate the impact of 1730_LTAN. By comparing EDA spread in denial and addition scenarios, we assess the potential benefit of adding 1730_LTAN observations and put the expected impact into context with impact achieved for real data. The latter allows cross-comparisons to traditional Observing System Experiments with real data, such as those of Duncan et al (2021).

To investigate the vertical extent of the impact, Figure 5 presents changes in EDA spread for geopotential height across three addition scenarios compared to the Baseline. Vertical profiles of EDA spread reduction for geopotential height are shown for both the southern hemisphere (latitude $> 20^{\circ}\text{S}$) and the northern hemisphere (latitude $> 20^{\circ}\text{N}$) for the period 8–30 June 2021. When assessing changes in the observing system, a positive impact arises when the ensemble spread is reduced, indicating improved analysis/forecast error statistics. The spread reductions in Baseline+1730_LTAN (green line) shows how 1730_LTAN data reduces forecast uncertainty over the two hemispheric regions. The reduction is comparable to the benefits currently achieved from existing MW-sounding instruments aboard NOAA's POES satellites (see dashed red line depicting the Baseline+POES experiment). The greatest improvements in forecast accuracy are observed when 1730_LTAN data is combined with data from POES satellites (Baseline+POES+1730_LTAN, purple line). Note that for our experimentation period, NOAA-18 has an LTAN of 22:00, close to that of the Metop satellites, whereas NOAA-15 and -19 have an LTAN of around 19:30, hence providing further complementary orbital coverage. The results for 1730_LTAN are qualitatively consistent with the experience with real data from MWHS-2 from FY-3E in the early-morning orbit (Steele et. al., 2023), which also shows a good impact of an early-morning satellite, including in the presence of POES satellites. These findings highlight the potential value of integrating 1730_LTAN into the future NOAA observation system to enhance global weather prediction capabilities.

In addition, two denial scenarios were conducted, and their EDA performances provide further context for the 1730_LTAN results (Figure 5). The results show that the spread reduction from 1730_LTAN is about a quarter of the spread increase resulting from the denial of all JPSS instruments in the “No JPSS” experiment (dashed grey). In other words, incorporating 1730_LTAN into NOAA’s JPSS system, as represented in the Baseline+1730_LTAN scenario, would enhance the overall impact of NOAA’s polar-orbiting systems by approximately 25%. Note, however, that the JPSS system has additional impacts, not captured by the EDA metrics considered here, such as for atmospheric chemistry or cross-calibration. The EDA spread reduction from 1730_LTAN is also sizeable compared to the spread increase from the loss of the two ATMS instruments in the 13:30 orbit (black line). The findings can be compared to OSEs about the continued benefit of adding MW sounders performed by Duncan et al (2021). Consistent with their results, we see a continued benefit from adding further MW-sounders, even though the rate of benefit reduces with an increasing number of satellites. It is interesting to note that the improvements in performance in the EDA between “No ATMS” and “No JPSS” cases can be attributed to the contribution of CrIS and VIIRS AMVs when they are added to ATMS.

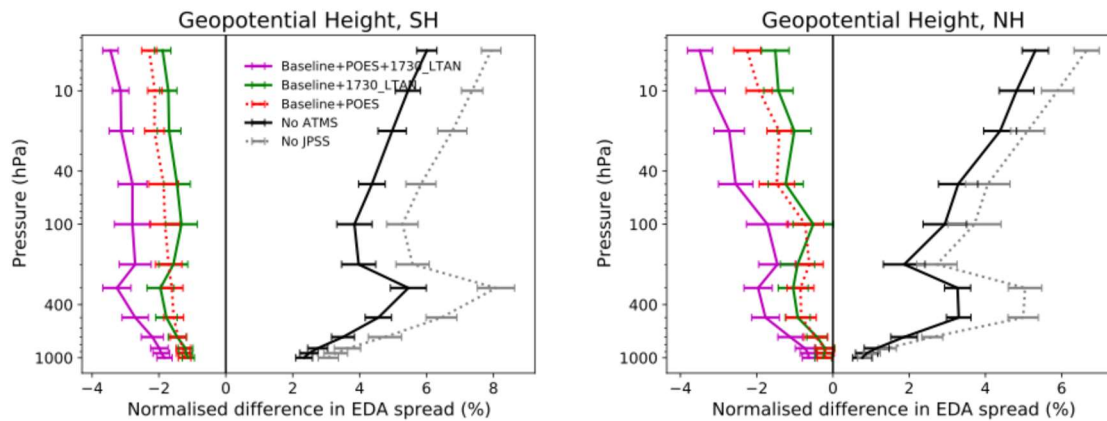


Figure 5: Vertical profiles of EDA spread reduction for geopotential height in the southern hemisphere (latitude $> 20^{\circ}\text{S}$), and northern hemisphere (latitude $> 20^{\circ}\text{N}$). The baseline observing system, which used as proxy for a future observing system without NOAA MW sounders, includes all non-MW observations used operationally at ECMWF in 2021, excluding passive MW data from China. For comparison, the denial from the baseline of all assimilated ATMS data from S-NPP and NOAA-20 is also shown. Data are for the period 8-30 June 2021 and error bars indicate an estimate of 95% confidence.

EDA spread reductions for other main atmospheric variables, such as temperature, relative humidity, and wind, have been assessed, and the impact of the 1730_LTAN data is similar to that seen for the geopotential. These reductions offer valuable insights into the broader benefits of 1730_LTAN for improving forecast accuracy. Figure 6 highlights vertical profiles of EDA spread reductions for temperature in both the Southern and Northern Hemispheres, showing improvements at various altitudes. Figure 6 demonstrates the positive impact of 1730_LTAN data on relative humidity and wind in the tropics. The impact is weaker in the tropics, in line with previous findings about MW-sounder impact both from OSEs with real data as well as EDA experimentation with simulated data (Duncan et al 2021, Lean et al 2022, 2023).

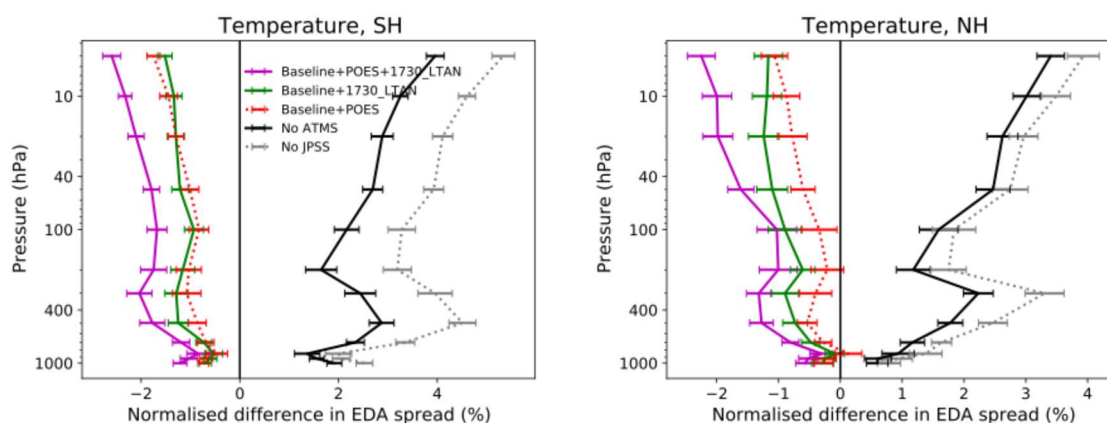


Figure 6: Same as Figure 5, but for Temperature in in the southern hemisphere (latitude > 20°S), and northern hemisphere (latitude > 20°N).

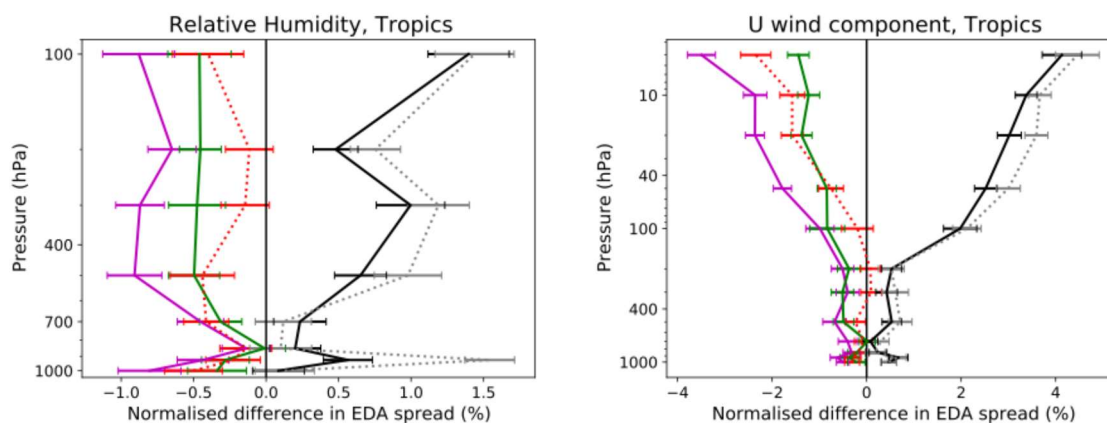


Figure 7: Same as Figure 5, but for Relative Humidity and U component of wind in the tropics (latitude ± 20°N). Relative humidity spread is shown up to 100 hPa, as humidity increments are not permitted above the hygropause.

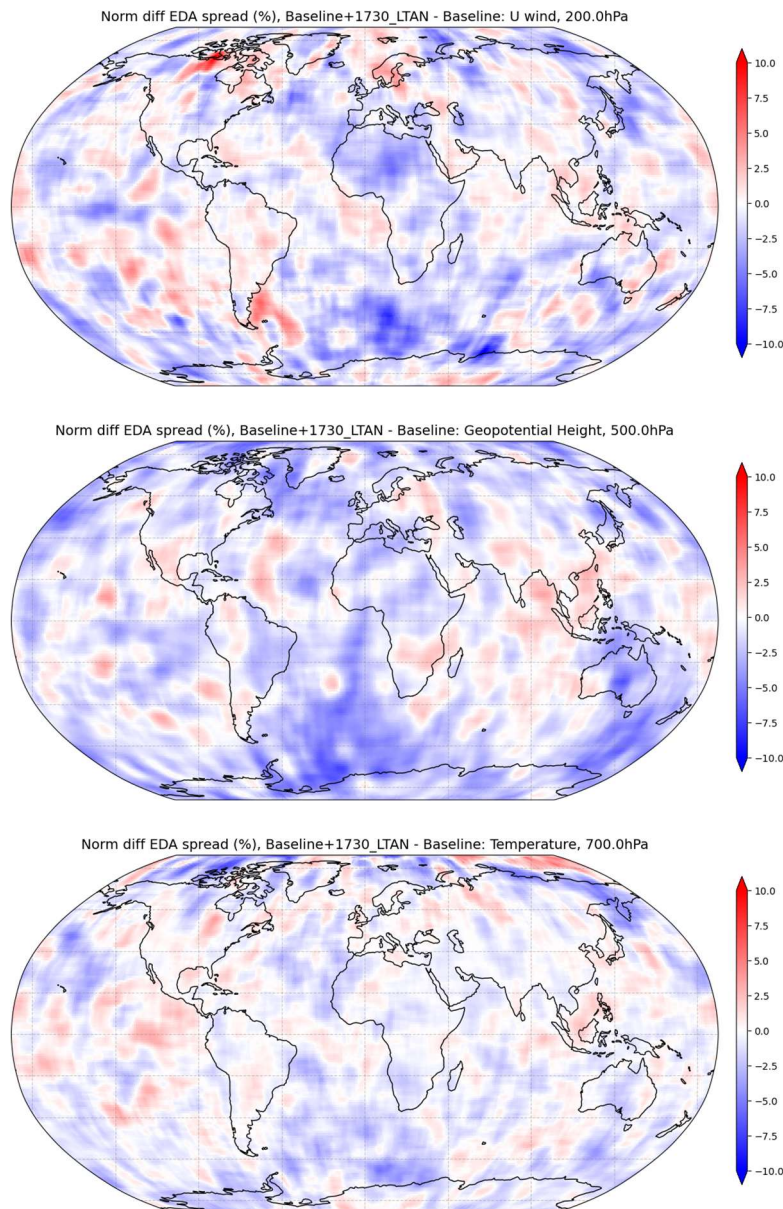


Figure 8: Maps showing the percentage difference in EDA spread between Baseline+1730_LTAN and the Baseline for U component of wind at 200 hPa (top panel), geopotential height at 500 hPa (middle panel) and temperature at 700 hPa (bottom panel). Blue colours indicate areas where EDA spread values are smaller in the Baseline+1730_LTAN scenario indicating benefit from the addition of the simulated 1730_LTAN data.

In the Baseline+1730_LTAN scenario presented in Section 4, all MW satellite data from the current JPSS ATMS (on S-NPP and NOAA-20) and a potential future instrument in the 1730 LTAN within the NOAA LEO system are assimilated into the EDA system. Figure 8 presents maps showing the percentage difference in EDA spread for this scenario of Baseline+1730_LTAN against Baseline. These maps are for three critical atmospheric variables: 1) the U component of wind at 200 hPa, 2) geopotential height at 500 hPa, and 3) temperature at 700 hPa. The maps use blue areas to represent reductions in EDA spread, indicating that the assimilation of the simulated 1730_LTAN data reduces forecast uncertainty. Notably, the most significant reductions, depicted in dark blue, are observed in the

polar regions, especially over Antarctica. Meanwhile, smaller but still notable reductions are seen in the tropics. This pattern highlights the impact of adding an ATMS instrument in the early-morning orbit.

These reductions in EDA spread emphasize the wide-ranging influence of 1730_LTAN data on atmospheric analyses. Furthermore, the analysis reveals that NWP systems have not yet reached a saturation point in terms of the benefits gained from adding additional microwave sounders beyond those in the Metop and JPSS orbits. This suggests that incorporating more MW sounders, like 1730_LTAN, can continue to yield significant improvements in forecast performance.

6.2. Sensitivity to the instrument noise performance

In this study, we have so far assumed an instrument noise performance for 1730_LTAN that is similar to that of the ATMS on S-NPP. As highlighted by Lean et al (2023), the instrument noise can play a critical role for the achievable impact in NWP, particularly for temperature-sounding channels, with a poorer instrument noise leading to a smaller impact and a better noise performance leading to a larger impact. To characterise this aspect for 1730_LTAN, we have conducted an additional EDA experiment in Table 7, in which we assume a poorer noise performance for the temperature-sounding channels. For this experiment, we increased the NEDT values used to specify the perturbations of the simulated observations after 3x3 averaging by 100% for channels 1-10 and by 50% for channels 11-15. The assigned clear-sky observation error values for these channels were also increased in a similar way. Where the increased clear-sky observation error then exceeds the cloudy observation error, the latter was adjusted accordingly. The settings simulate a hypothetical poorer noise performance, to test the sensitivity of our results to this parameter.

Table 7: A detailed list of scenarios in the instrument noise sensitivity experiments.

Scenario Name	Observing system other than MW sounding	MW sounding in 9:30 orbit	MW sounding in 13:30 orbit	MW sounding in 17:30 orbit	Further MW sounding
Baseline (Same as that in Table 5)	Full	Two Metop	Two ATMS (S-NPP, NOAA-20)	-	-
Baseline+1730_LTAN (Same as that in Table 5)	Full	Two Metop	Two ATMS (S-NPP, NOAA-20)	1730_LTAN (with S-NPP like noise levels)	-
Baseline+1730_LTAN_degraded_noise	Full	Two Metop	Two ATMS (S-NPP, NOAA-20)	1730_LTAN (with a degraded noise performance)	-

An additional EDA experiment, referred to as `Baseline+1730_LTAN_degraded_noise`, was performed using this degraded noise instrument. This scenario is detailed alongside the `Baseline+1730_LTAN` scenario in Table 5. By comparing the spread reductions from `Baseline+1730_LTAN` and `Baseline+1730_LTAN_degraded_noise` against the Baseline scenario, we evaluated the impact of poorer instrument noise on the assimilation of microwave observations and its overall effect on NWP performance.

Figures 9-11 illustrate the vertical profiles of EDA spread reduction for temperature and geopotential height in both northern and southern hemispheres, and relative humidity and U wind components in the tropics resulting from adding the S-NPP-like ATMS (green line) or the more poorly performing ATMS (red) to the Baseline. The results show that while the degraded noise instrument still contributes positively to NWP, the overall impact of `Baseline+1730_LTAN_degraded_noise` is significantly worse compared to `1730_LTAN` with ATMS-like performance on S-NPP. This difference is particularly evident in temperature and geopotential height, where the most pronounced improvements occur above 500 hPa, highlighting the sensitivity of these variables to instrument noise performance. For humidity in the troposphere, the impact is similar for the two noise scenarios (e.g., Fig. 11), reflecting that the performance of the humidity-sounding channels is unaltered.

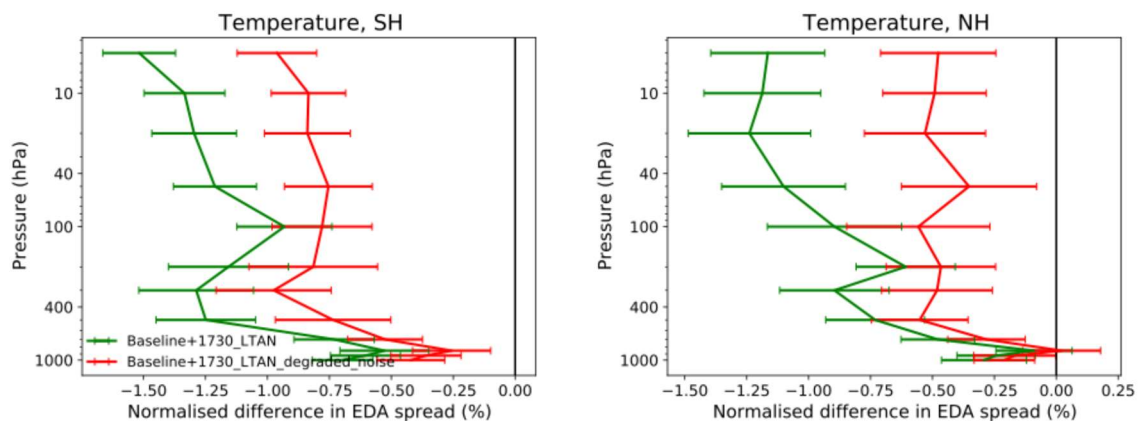


Figure 9: Vertical profiles of EDA spread reduction for temperature in the southern and northern hemisphere from the different instrument noise scenarios.

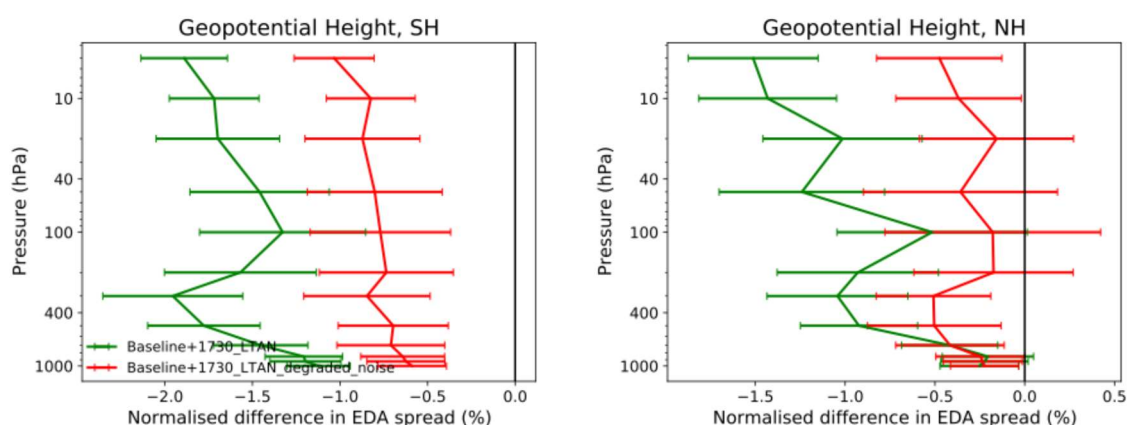


Figure 10: Same as Figure 9, but for geopotential height.

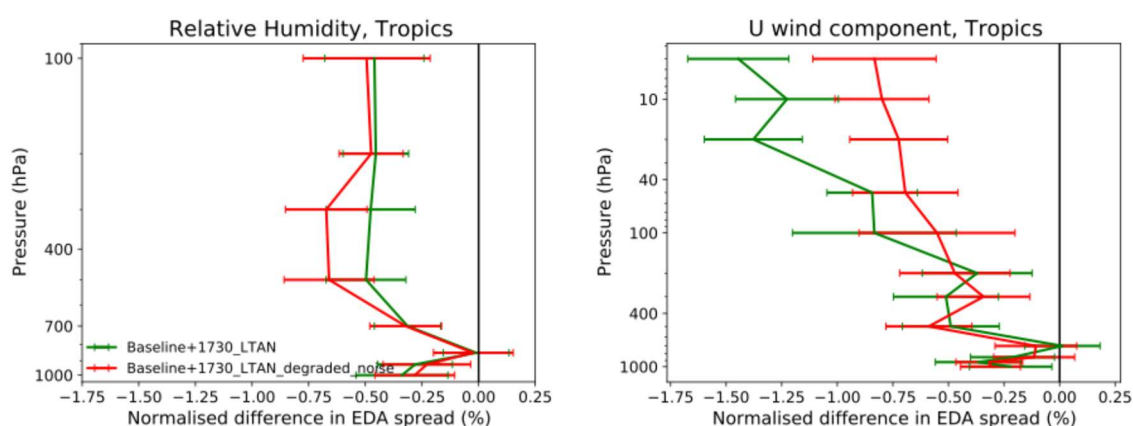


Figure 11: Same as Figure 9, but for Relative Humidity and U component of wind in the tropics.

7. Conclusion and Future Plans

The Ensemble of Data Assimilations (EDA) method has been established as a powerful tool for assessing the potential impact of future observations on analysis and short-range forecast errors. Using simulated new observations combined with real observations from existing systems, the EDA evaluates how the spread of the ensemble evolves as these new data are added. Here we perform EDA experiments for 1730_LTAN, that is, a hypothetical future ATMS instrument in 17:30 LTAN orbit, to evaluate the expected NWP benefit from such a future system. To simulate the 1730_LTAN impact, we assume that the data quality is comparable to that of the S-NPP ATMS.

The new observations were first simulated based on realistic atmospheric representations, using ECMWF's high-resolution analysis. Perturbations were added to the simulated data to replicate expected instrument noise. A cross-check was performed to ensure the accuracy of the 1730_LTAN data simulation before executing a series of EDA scenarios. Two denial and three addition EDA scenarios were carried out in the IFS system (Cycle 48r1), incorporating ATMS data assimilation in all-sky conditions over the period from 1 to 30 June 2021.

The results demonstrate that adding 1730_LTAN MW data significantly improves forecasting accuracy, reducing EDA spread and enhancing signal detection compared to existing configurations. The findings suggest that 1730_LTAN has an expected impact comparable to that of the old POES satellites when added to a system with MW-sounding from the 9:30 and 13:30 orbits only. The size of this impact using the measures presented here is about a quarter of the combined impact from ATMS, CrIS and AMVs from two satellites of the JPSS system. This highlights how both 1730_LTAN and the remaining POES instruments significantly add to the impact achieved from US systems. Best results are obtained when both 1730_LTAN and POES satellites are used together. These outcomes are consistent with previous ECMWF studies (e.g., Lean et al 2022, 2023), which suggest that NWP systems have not yet reached saturation from the addition of MW sounders beyond Metop and JPSS orbits. The findings are also qualitatively consistent with the experience gained with data from the early-morning FY-3E satellite, which shows a significant positive impact in global NWP (Steele et al 2023, Xiao et al 2023). It should be emphasised, however, that the impact estimates obtained here assume an instrument performance comparable to that of the ATMS instrument on S-NPP.

Sensitivity experiments demonstrate that the impact of 1730_LTAN will be reduced if the instrument noise performance is worse than that of S-NPP. While the 1730_LTAN instrument with degraded noise performance still provides a positive impact on NWP, the overall benefit is significantly reduced compared to the ATMS-like noise levels on S-NPP. In particular, the temperature-sounding channels are more affected by the poorer noise performance, resulting in a noticeable reduction in the spread reduction for atmospheric variables. These findings highlight the importance of instrument noise characteristics in determining the overall performance of microwave observations in NWP systems.

The consistency between EDA spread-reductions obtained with real and simulated ATMS data was also investigated, showing overall good agreement. This is an important result, as it confirms that the EDA experiments with our simulated ATMS data provide a reliable indication of EDA spread reduction achieved with real data. This adds further confidence in the EDA spread estimates obtained for future observations. Using experiments with real data, Lean et al (2021a) previously also showed that there is a clear link between EDA spread reductions and forecast error reduction obtained in OSEs. Combining these two findings further underscores that the EDA-based impact estimates for MW sounders provide useful guidance for the forecast impact expected from such future systems.

As the microwave instrument in NOAA's next-generation NEON program, SMBA will introduce additional channels at 118 GHz and 229 GHz frequencies, compared to JPSS ATMS. These new channels are expected to enhance the accuracy and resolution of atmospheric observations, particularly for temperature and humidity profiling. Ongoing simulation of the SMBA instrument and its associated impact within the EDA system will play a critical role in future assessments. Particular attention will be given to how SMBA data can complement and enhance existing MW observation systems like those on Metop, JPSS, and future NOAA instruments. These simulations will help determine how the added channels improve the vertical resolution and sensitivity to key atmospheric parameters, which are essential for better capturing weather dynamics.

8. Acknowledgements

This study was supported by NOAA grants NA24NESX432C0001 and NA19NES4320002 (Cooperative Institute for Satellite Earth System Studies -CISESS) at the University of Maryland/ESSIC. Thanks to Joerg Ackermann for generating ATMS or ‘ATMS like’ scan simulations in this study. Thanks to Tony McNally for reviewing the manuscript.

9. References

Atlas, R.; Hoffman, R.; Ma, Z.; Emmitt, G.; Wood, S.; Greco, S.; Tucker, S.; Bucci, L.; Annane, B.; Hardesty, R.M.; et al., 2015: Observing System Simulation Experiments (OSSEs) to Evaluate the Potential Impact of an Optical Autocovariance Wind Lidar (OAWL) on Numerical Weather Prediction. *J. Atmos. Ocean. Technol.* 32, 1593–1613.

Baordo, F., Geer, A., 2016. Assimilation of SSMIS humidity-sounding channels in all-sky conditions over land using a dynamic emissivity retrieval. *Q.J.R.M.S.*, 2854–2866 <https://doi.org/10.1002/qj.2873>.

Biswas, Sayak & Kunkee, David & Poe, Gene & Swadley, Steven & Hong, Ye. (2024). 1/ f -Noise Estimation From Microwave Imager Data With Periodic Gaps. *IEEE Journal of Selected Topics in Applied Earth Observations and Remote Sensing*. PP. 1-16. 10.1109/JSTARS.2024.3456034.

Bonavita, M., E. Hólm, L. Isaksen, and M. Fisher, 2016: The evolution of the ECMWF hybrid data assimilation system. *Q. J. R. Meteorol. Soc.*, 142, 287-303, doi:10.1002/qj.265

Bormann, N., A. Fouilloux, W. Bell, 2013: Evaluation and assimilation of ATMS data in the ECMWF system. *J. Geophys. Res.*, 118(23), doi: 10.1002/2013JD020325

Bormann, N., H. Lawrence, J. Farnan, 2019: Global observing system experiments in the ECMWF assimilation system. ECMWF Technical Memorandum 839, 24pp, <https://www.ecmwf.int/node/18859>, doi: 10.21957/sr184iyz.

Bormann, N., Healy, S., Lean, K. & Lonitz, K. (2023) Predicting the forecast impact of potential future observing systems. *ECMWF Newsletter*, 174, 12–17.

di Tomaso, E. and Bormann, N., 2011: Assimilation of ATOVS radiances at ECMWF: first year EU-METSAT fellowship report. Shinfield Park, Reading, URL <https://www.ecmwf.int/node/9049>.

Duncan, D.I., Bormann, N. & Hólm, E.V., 2021: On the addition of microwave sounders and numerical weather prediction skill. *Q J R Meteorol Soc*, 147, 3703–3718. doi: 10.1002/qj.4149

Errico, R. M. and N. C. Privé, 2018: Some general and fundamental requirements for designing observing system simulation experiments (OSSEs). *World Weather Research Programme*, 2018-8, 24pp, <https://ntrs.nasa.gov/api/citations/20190025338/downloads/20190025338.pdf>

Geer, A.J. and Bauer, P. (2011), Observation errors in all-sky data assimilation. *Q.J.R. Meteorol. Soc.*, 137: 2024-2037. <https://doi.org/10.1002/qj.830>

Geer, A.J., F. Baordo, N. Bormann, P. Chambon, S.J. English, M. Kazumori, H. Lawrence, P. Lean, K. Lonitz, C. and Lupu, 2017: The growing impact of satellite observations sensitive to humidity, cloud and precipitation. *Q J R Meteorol Soc*, 143: 3189-3206. doi: 10.1002/qj.3172

Geer, A.J., P. Bauer, K. Lonitz, V. Barlakas, P. Eriksson, J. Mendrok, A. Doherty, J. Hocking, and P. Chambon, 2021: Bulk hydrometeor optical properties for microwave and sub-millimetre radiative transfer in RTTOV-SCATT v13.0. *Geosci Model Dev*, 14, 7497–7526, doi: 10.5194/gmd-14-7497-2021

Grody, N., Zhao, J., Ferraro, R., Weng, F., , Boers, R., 2001. Determination of precipitable water and cloud liquid water over oceans from the NOAA 15 advanced microwave sounding unit. *J. Geophys. Res.*, 2943–2953, doi:10.1029/2000JD900616.

Harnisch, F., S. B. Healy, P. Bauer, S. J. English, 2013: Scaling of GNSS Radio Occultation Impact with Observation Number Using an Ensemble of Data Assimilations. *Mon Wea Rev*, 141, 4395–4413. doi: 10.1175/MWR-D-13-00098.1.

Healy, S.B., Lean, K., Semane, N., Bormann, N., 2023. Task 2: Doppler Wind Lidar EDA Impact Assessment. EUMETSAT Contract EUM/CO/22/4600002673/SDM Final Report, ECMWF, Reading, UK.

Healy, S. B., N. Bormann, A. Geer, E. Hólm, B. Ingleby, K. Lean, K. Lonitz and C. Lupu, 2024: Methods for assessing the impact of current and future components of the global observing system. ECMWF Technical Memorandum 916, doi: 10.21957/2f240fe55f

Isaksen, L, Bonavita, M, Buizza, R, Fisher, M, Haseler, J, Leutbecher, M, Raynaud, L, 2010: Ensemble of data assimilations at ECMWF. ECMWF Technical Memorandum 636, <https://www.ecmwf.int/node/10125>, doi: 10.21957/obke4k60, 48pp

Kalluri, S., et al, 2021: Satellite Microwave Sounding Measurements in Weather Prediction: A Report of The Virtual NOAA Workshop on Microwave Sounders. NOAA Technical Report NESDIS 155, doi: 10.25923/WKGD-PW75, 25pp.

Karbou, F., Gérard, E., Rabier, F., 2006. Microwave land emissivity and skin temperature for AMSU-A and -B assimilation over land. *QJRM* 132, 2333–2355.

Kazumori, M., English, S.J., 2015. Use of the ocean surface wind direction signal in microwave radiance assimilation. *QJRM* 141, 1354–1375. URL: <https://rmets.onlinelibrary.wiley.com/doi/abs/10.1002/qj.2445>, doi:10.1002/qj.2445.

Kim E., C.-H. J. Lyu, K. Anderson, R. V. Leslie, and W. J. Blackwell (2014). S-NPP ATMS instrument prelaunch and on-orbit performance evaluation. *Journal of Geophysical Research, Atmosphere*, vol. 119, no. 9, pp. 5653–5670.

Lang, S., E. Hólm, M. Bonavita & Y. Trémolet, 2019: A 50-member Ensemble of Data Assimilations, ECMWF Newsletter No. 158, 27–29.

Lawrence, H., N. Bormann, A.J. Geer, Q. Lu, S.J. English, 2018: Evaluation and assimilation of the Microwave Sounder MWHS-2 onboard FY-3C in the ECMWF Numerical Weather Prediction System. *IEEE Trans Geosci Remote Sensing*, 56, 3333-3255, doi: 10.1109/TGRS.2018.2798292

Lean, K., N. Bormann, S.B. Healy, 2021a: Calibration of EDA spread and adaptation of the observation error model. ESA Contract Report for 4000130590/20/NL/IA, 23pp, <https://www.ecmwf.int/node/20302>, doi: 10.21957/1auh0nztg

Lean, K., N. Bormann, S.B. Healy, 2021b: Developing a flexible system to simulate and assimilate small satellite data. ESA Contract Report for 4000130590/20/NL/IA, 18pp, <https://www.ecmwf.int/node/20303>, doi: 10.21957/kjmxyh9xy

Lean, K., N. Bormann, S.B. Healy, S. English, 2022: Final Report: Study to assess earth observation with small satellite and their prospects for future global numerical weather prediction. ESA Contract Report for 4000130590/20/NL/IA, 40pp, <https://doi.org/10.21957/kp7z1sn1n>

Lean, K., N. Bormann, S.B. Healy, 2023: Evaluation of initial future EPS-Sterna constellations with 50 and 183 GHz. EUMETSAT contract report for EUM/CO/22/4600002673/SDM, 34pp, <https://doi.org/10.21957/0a695fcc39>

Ma, Z., L. P. Riishøjgaard, M. Masutani, J. S. Woollen, and G. D. Emmitt, 2015: Impact of Different Satellite Wind Lidar Telescope Configurations on NCEP GFS Forecast Skill in Observing System Simulation Experiments. *J. Atmos. Oceanic Technol.*, 32, 478–495, <https://doi.org/10.1175/JTECH-D-14-00057.1>.

Qin, Z., X. Zou, and F. Weng (2013), Analysis of ATMS striping noise from its Earth scene observations, *J. Geophys. Res. Atmos.*, 118, 13,214–13,229, doi:10.1002/2013JD020399.

Saunders, R., Hocking, J., Turner, E., Havemann, S., Geer, A., Lupu, C., Vidot, J., Chambon, P., Köpken-Watts, C., Scheck, L., Stiller, O., Stumpf, C., Borbas, E., 2020. RTTOV-13 science and validation report. EUMETSAT NWP SAF, version 1.0 URL: <https://nwp-saf.eumetsat.int/site/software/rttov/documentation/>.

Steele, L., N. Bormann, D. Duncan, 2023: Assimilating FY-3E MWHS-2 observations, and assessing all-sky humidity sounder thinning scales. EUMETSAT/ECMWF Fellowship Programme Research Report 62, 31pp, <https://doi.org/10.21957/f42a9d9542>

Tan, D. G. H., E. Andersson, M. Fisher, and L. Isaksen, 2007: Observing-system impact assessment using a data assimilation ensemble technique: Application to the ADM-Aeolus wind profiling mission. *Q J R Meteorol Soc*, 133, 381–390.

Weston, P., and N. Bormann, 2018: Enhancements to the assimilation of ATMS at ECMWF: Observation error update and addition of NOAA-20. EUMETSAT/ECMWF Fellowship Programme Research Report No 48, 28pp, <https://www.ecmwf.int/en/elibrary/80916-enhancements-assimilation-atms-ecmwf-observation-error-update-and-addition-noaa>

Xiao, H., Han, W., Zhang, P., & Bai, Y. (2023). Assimilation of data from the MWHS-II onboard the first early morning satellite FY-3E into the CMA global 4D-Var system. *Meteorological Applications*, 30(3), e2133. <https://doi.org/10.1002/met.2133>